WYLE LABORATORIES - RESEARCH STAFF

REPORT WR 67- 10

RESPONSES OF RECTANGULAR PANELS TO RANDOM ACOUSTIC EXCITATIONS BY MECHANICAL IMPEDANCE MEASUREMENT TECHNIQUES

by

G. C. Kao

Submitted as a Summary Report Under Contract NAS8-5384, Task 16

"Simple Panel Impedance Measurement Program"

Prepared by G. C. Kao

G. C. Kao
Program Manager

Approved by L. C. Sutherland

L. C. Sutherland
Director of Research Staff, Huntsville

Date June, 1967

COPY NO. 1

FOREWORD

The research project presented in this report was performed by Wyle Laboratories, Huntsville, Alabama, for the Vibration and Acoustic Branch, P and VE Laboratory, Marshall Space Flight Center, Huntsville, Alabama, under Contract NAS8-5384, Task 16, "Simple Panel Impedance Measurement Program." Mr. R. Jewell, Chief, Advanced Methods and Research Section, P and VE, MSFC, was the contract monitor. The research task was performed during the period of July 1966 through June 1967 under the supervision of Mr. L. Sutherland, Director of Research, Wyle Laboratories, Huntsville Test Facility, and Dr. G.C. Kao was the Principal Investigator.

The author is indebted to Messrs. L. Sutherland, R. White, D. Bozich and F. Murray of Wyle Laboratories for their valuable advice and assistance throughout the period of performance of this task. He also wishes to acknowledge with gratitude the encouragement and support of this program by Mr. R. Jewell of MSFC.

ABSTRACT

Analytical development of mechanical impedance measurement techniques to predict responses of linear structures to random acoustic excitations is presented in this report. The investigation shows that the point impedance and the transfer impedance data of complex structures could be used to compute frequency-average mode shapes and joint acceptance functions; these quantities could, then, be used to predict structural responses.

Three rectangular aluminum panels were tested in this program. Mechanical impedance measurements and acceleration response data to sinesweep and random acoustic excitations were obtained. The Wyle analog-Digital data acquisition system, which was developed under a similar impedance research program (NAS8-11262), was used for all tests. Comparison of analytical and experimental results will be presented in a subsequent report.

TABLE OF CONTENTS

LIST OF TABLES

LIST OF FIGURES

LIST OF SYMBOLS

A	=	surface area
f	=	frequency
f_c	=	band center frequency
f_{k_u}, f_{k_L}	=	upper and lower limit frequencies of a frequency band
F_o	=	amplitude of exciting force
$F(t)$	=	forcing function
$H(i\omega)$	=	mechanical mobility or frequency response function
H_r^s	=	acceleration-to-force ratio (or frequency response function)
i	=	$\sqrt{-1}$
$J^2_{mn}(\omega)$	=	joint acceptance function
k_m	=	generalized stiffness
M_m	=	generalized mass
p_o	=	reference pressure
Q	=	dynamic magnification factor
Q_m	=	generalized dynamic magnification factor
$\vec{r}, \vec{s}$	=	space vectors
$Z(i\omega)$	=	mechanical impedance
$Z^*(i\omega)$	=	complex conjugate of $Z(i\omega)$
$Z_m(i\omega)$	=	generalized modal impedance

LIST OF SYMBOLS (CONTINUED)

Greek Symbols

α	=	acoustic mobility function
δf	=	incremental bandwidth in Hz.
Δf	=	bandwidth in Hz.
$[\,]_{\Delta f}$ or $\|\,\|_{\Delta f}$	=	frequency average quantities
$\dot{\xi}$	=	velocity response
$\ddot{\xi}$	=	acceleration response
$\xi(t)$	=	displacement response
ϕ_m	=	m^{th} normal mode
Φ	=	response power spectral density
ω	=	exciting frequency
ω_m	=	m^{th} natural frequency
ω_o	=	natural frequency of a single-degree-of-freedom system
ρ	=	surface mass density

1.0 INTRODUCTION

The purpose of this research program is to investigate the feasibility of applying mechanical impedance measurement techniques for predicting dynamic responses of structures to acoustic excitations.

Dynamic responses of a linear elastic structure, in general, could be expressed in terms of normal modes of the structural system provided that its mode shapes and natural frequencies could be predetermined. The mode shapes and corresponding natural frequencies of a structure could be determined from the equations of motion of free vibration; the true mode shapes would, of course, contain all the dynamic characteristics of the system, i.e., boundary conditions, structural damping, radiation damping, structural geometries, etc. However, solutions to equations of free vibration of structures have been limited to simple structures with well defined boundary conditions, such as simply supported beams and plates. Mathematical methods to find satisfactory mode shapes for complex structures have not been successful due to complexities of structural configurations and some uncertainties about material properties and boundary conditions. In order to find approximate solutions for responses of complex structures, crude approximations on structural geometries, material properties and boundary conditions have been used to formulate mathematical models that would yield tractable equations of motion. Thus, the accuracies of such solutions are doubtful.

The advance of measurement techniques for forcing and response signals coupled with the use of analog/digital data acquisition systems, makes it possible to obtain true mode shapes of a structure by carefully planned experimental programs. A practical method to obtain mode shapes of a structure involves applying a concentrated sinusoidal point force at a point on the structure and monitoring response signals (i.e., accelerometer signals) at other locations on the structure. At low frequencies of vibration, the mode shape could be determined experimentally at each resonant frequency. The force-to-response ratios are defined as the mechanical impedance of the structure at the measured points. These functions, as will be shown in the latter analysis, define the dynamic characteristics of the structure. Information on mode shapes and the resistance function of the tested structure could be obtained from the measured impedance signals.

This report presents a combined analytical and experimental approach to obtain responses of structures to acoustic excitations with measured impedance information. The analysis begins with the response of a single-degree-of-freedom system, in which the mechanical impedance, in its simplest form, is introduced. The analysis of a continuous system to a discrete sinusoidal loading is presented next; the general expressions for the driving point impedance and the transfer impedance are formulated. With this information available, the general expressions of response power spectral density to random acoustic excitations are derived. Details of these developments together with an experimental verification program will be presented in the following sections.

2.0 STRUCTURAL RESPONSE TO ACOUSTIC EXCITATION

In this section, the formulation of a systematic response prediction technique to acoustic excitations is presented. The force-to-response expressions for a single-degree-of-freedom system as well as for a continuous system have been utilized to formulate expressions for frequency-average quantities used for predicting vibro-structural responses. Consider first, however, the following brief review of previous investigations on prediction of vibro-acoustic response.

2.1 Previous Investigations

Research effort in prediction methods for structural acoustic response tends to fall into three categories, namely, the analytical, the energy and the empirical approaches.

The analytical approach follows the formulation of classical equations of motion and then seeks to find solutions for these differential equations. Such an approach is usually limited to restricted classes of simple structures whose normal modes can be determined with relatively simple mathematical manipulation. A typical treatment of this kind has been documented by Smith and Lyon [1]*, which contains an extensive bibliography of most of the up-to-date information on analytical approaches to vibro-acoustic response problems. In addition to [1], some simple plate response problems were discussed by Lyon [2], Maidanik [3], Powell [5, 6, and 7], Bozich [8], and the response of cylindrical shells was investigated by Wenzel [9], White [10] and Dyer [14]. However, the necessity of knowing the normal modes of a structure, indeed, limit the scope of application of such approaches.

The precise determination of structural responses to random acoustic excitation is impossible and impractical, rather, the average response magnitudes would be of prime interest. The energy approach attempts to evaluate mean-square responses of structures based on the average number of modes existing in a frequency interval (or so called modal density concept), and to avoid using any particular mode shape. Such an approach simplifies, significantly, the mathematical manipulations involved in obtaining response equations. Examples on application of the energy approach can be found on published papers by Smith and Lyon [1], Lyon and Maidanik [4], Heckl et al. [11], Lyon [12], Dyer [15] and Franken and Lyon [16]. This method sometimes requires actual data of the disspipation function which must be obtained from measurements of real structures; such work can be found in reports by Heckl [13] and Franken and Lyon [16].

---

* Numeral(s) appearing inside brackets refer to the reference source(s) defined in the Reference Section.

The empirical approach is based on the knowledge gained through the studies of simple structures and coupled with statistical treatment of measured data to formulate a set of equations suitable for practical application. Recently, the concept of mechanical impedance (or the force-to-response ratio) has been applied in determining dynamic characteristics of structures by Kao et al. [18] and White et al. [19] and efforts have been to relate the measured data of a structure with the measured acoustic data to predict responses. Considerable work has been done by Bozich and Sutherland [20] on applying on-line data acquisition system to process and reduce test data to a usable form for vibro-acoustic response predictions.

The vibro-acoustic literature discussed in this section does not present an exhaustive search of all pertinent information in this area; rather, the main purpose is to demonstrate the attempts of various research organizations in unlocking the mysteries of sound - structural vibration problems to refine design techniques for complex launch vehicles.

The research program described in this report presents a systematic method for utilizing digital data acquisition techniques to extract information on mode shapes and mechanical impedance functions of structures in order to predict responses of a complex structure to acoustic excitations.

2.2 Response of a Single-Degree-of-Freedom System

The response of a single-degree-of-freedom system, as shown in Figure 2.1, with mass, m, stiffness, k, viscous coefficient, c, and sinusoidal load, F_o, can be shown [21] to be

$$\xi(t) = \frac{F_o e^{i\omega t}}{k\left[1 - \left(\frac{\omega}{\omega_o}\right)^2 + \frac{i}{Q}\frac{\omega}{\omega_o}\right]} \qquad (2.1)$$

where

$\xi(t)$ = displacement response

$\omega_o = \sqrt{\frac{k}{m}}$ = natural frequency

$Q = \frac{m\omega_o}{c}$ = dynamic magnification factor

F_o = amplitude of the exciting force

ω = exciting frequency

$i = \sqrt{-1}$.

Equation (2.1) can be written as

$$\xi(t) = \frac{F(t)}{Z(i\omega)} \tag{2.2}$$

or

$$\xi(t) = F(t) \cdot H(i\omega) \tag{2.3}$$

where $$Z(i\omega) = k\left[1 - \left(\frac{\omega}{\omega_o}\right)^2 + \frac{i}{Q}\left(\frac{\omega}{\omega_o}\right)\right] \tag{2.4}$$

and

$$H(i\omega) = Z(i\omega)^{-1} \tag{2.5}$$

$Z(i\omega)$ and $H(i\omega)$ are defined, respectively, as the mechanical impedance and mobility (or frequency response function) of the single-degree-of-freedom system.

The expressions for equations (2.4) and (2.5) bear special meaning in later analyses, because the response equation, as will be shown in the next section, contains similar expressions for each modal vibration regardless of the locations of exciting forces. This indicates that the impedance quantity $Z(i\omega)$ or its inverse $H(i\omega)$ are the common factors representing structural resistance functions which are independent of locations of exciting forces.

2.3 Response of a Continuous Linear Elastic System

The response of a continuous linear elastic system, as shown in Figure 2.2, to a sinusoidal point force $F(t)$, at $\vec{s}$, can be shown [21] to have the following ratio:

$$\frac{\xi(\vec{r}, \vec{s}, \omega)}{F(t)} = \sum_m \frac{\phi_m(\vec{r})\,\phi_m(\vec{s})}{Z_m(i\omega)} \tag{2.6}$$

where

$F(t) = F_o \sin \omega$

ϕ_m = m-th normal mode shape

$\vec{r}, \vec{s}$ = space vectors which locate points $\vec{r}$ and $\vec{s}$ in the system

Z_m = modal impedance

$$= k_m \left[1 - \left(\frac{\omega}{\omega_m}\right)^2 + \frac{i}{Q_m} \left(\frac{\omega}{\omega_m}\right) \right] \tag{2.7}$$

k_m = generalized stiffness

ω_m = m-th natural frequency $= \sqrt{\frac{k_m}{M_m}}$

M_m = generalized mass $= \int_s \rho(\vec{s})\, \phi_m^2(\vec{s})\, d\vec{s}$

Q_m = generalized dynamic magnification factor.

ρ = surface mass density.

Equation (2.6) is a general transfer mobility expression, and by interchanging the sequence of $\vec{r}$, and $\vec{s}$ in equation (2.6) the following relationship is obtained:

$$\xi(\vec{r}, \vec{s}, \omega) = \xi(\vec{s}, \vec{r}, \omega) \tag{2.8}$$

Equation (2.8) is the statement of Maxwell's reciprocal theorem in a dynamic sense.

The expressions for velocity and acceleration at $\vec{r}$ due to a periodic point load, F(t), at $\vec{s}$ can be deduced from equation (2.6) as:

$$\dot{\xi}(\vec{r}, \vec{s}, \omega) = i\omega\, \xi(\vec{r}, \vec{s}, \omega) \tag{2.9}$$

$$\ddot{\xi}(\vec{r}, \vec{s}, \omega) = -\omega^2\, \xi(\vec{r}, \vec{s}, \omega) \tag{2.10}$$

The acceleration-to-force ratio, which is most adaptable for experimental measurements, is defined as the acceleration mobility and expressed by:

$$H_r^s(\ddot{\xi}, i\omega) = \frac{\ddot{\xi}(\vec{r}, \vec{s}, \omega)}{F(t)} = -\omega^2 \sum_m \frac{\phi_m(\vec{r})\, \phi_m(\vec{s})}{Z_m(i\omega)} \tag{2.11}$$

The expression for point mobility is obtained by replacing all the $\vec{s}$ in equation (2.11) with $\vec{r}$, thus

$$H_r^r(\ddot{\xi}, i\omega) = -\omega^2 \sum_m \frac{\phi_m^2(\bar{r})}{Z_m(i\omega)} \qquad (2.12)$$

Equations (2.11) and (2.12) will be used in the subsequent section to derive equations suitable for extracting useful information for predicting responses.

2.4 Application of Point Mobility Measurements

The proposed method in utilizing point mobility measurements centers on a digital technique developed previously by Bozich [20], in which the average mean square value of a mobility function, which has been evaluated at several discrete frequencies within a frequency band, Δf, can be obtained by multiplying each discrete value of the function, i.e., at frequency f, by an incremental bandwidth δf, and summing up all the subsequent sets of values over the bandwidth Δf, and expressing this final quantity at the center frequency of the band f_c. Therefore, the mean-square value of the mobility function over a bandwidth of Δf, may be expressed as follows:

$$\left[\left| H_r^s(\ddot{\xi}, f_c) \right|^2 \right]_{\Delta f} = \frac{1}{\Delta f} \sum_{k=k_L}^{k_u} \left| H_r^s(\ddot{\xi}, f_c) \right|^2 \delta f_k \qquad (2.13)$$

where

$\Delta f = f_{k_u} - f_{k_L}$, bandwidth in hertz

$\delta f_k = f_{k+1} - f_k$, incremental bandwidth in hertz

f_{k_u}, f_{k_L} = upper and lower limit frequencies of the band, respectively.

f_c = band center frequency.

The reason for using the frequency-average value rather than the discrete-frequency value is due to over-lapping of modes at high frequency of vibration, in which individual mode shapes could not be separated in the recorded signals. Thus equation (2.13) provides an expression which represents a pseudo equivalent mode $\phi(f_c)$, with pseudo resonant frequency, f_c.

Returning to equation (2.11), the quantity $\left|H_r^s(\ddot{\xi}, i\omega)\right|^2$ may be expressed as follows:

$$\left|H_r^s(\ddot{\xi}, f)\right|^2 = (2\pi f)^4 \sum_m \sum_n \frac{\phi_m(\bar{r})\ \phi_n(\bar{r})\ \phi_m(\bar{s})\ \phi_n(\bar{s})}{Z_m(f)\ Z_n^*(f)} \qquad (2.14)$$

Where $Z_n^*(f)$ is the complex conjugate of $Z_n(f)$. (Note that the imaginary number, i, has been omitted for brevity.)

If damping is relatively small in equation (2.14), cross-product terms can be neglected and a simplified expression of equation (2.14) may be written as:

$$\left|H_r^s(\ddot{\xi}, f)\right|^2 \simeq (2\pi f)^4 \sum_m \frac{\phi_m^2(\bar{r})\ \phi_m^2(\bar{s})}{\left|Z_m(f)\right|^2} \qquad (2.15)$$

Equation (2.15) is an approximate expression of transfer mobility at $\bar{r}$ due to a sinusoidal point load at $\bar{s}$. Similarly, the driving point mobility at $\bar{s}$ and $\bar{r}$ can be expressed, respectively, by equations (2.16) and (2.17) as follows:

$$\left|H_s^s(\ddot{\xi}, f)\right|^2 \simeq (2\pi f)^4 \sum_m \frac{\phi_m^4(\bar{s})}{\left|Z_m(f)\right|^2} \qquad (2.16)$$

$$\left|H_r^r(\ddot{\xi}, f)\right|^2 \simeq (2\pi f)^4 \sum_m \frac{\phi_m^4(\bar{r})}{\left|Z_m(f)\right|^2} \qquad (2.17)$$

Equations (2.15) through (2.16) could be expressed in terms of frequency-average quantities, as defined by equation (2.13), by the following expressions:

$$\left|H_r^s(\ddot{\xi}, f_c)\right|_{\Delta f}^2 \simeq (2\pi f_c)^4 \frac{\left[\phi^2(\bar{r}, f_c)\right]_{\Delta f} \left[\phi^2(\bar{s}, f_c)\right]_{\Delta f}}{\left[Z(f_c)\right]_{\Delta f}^2} \qquad (2.18)$$

$$\left| H_s^s(\bar{\xi}, f_c) \right|_{\Delta f}^2 \simeq (2\pi f_c)^4 \frac{\left[\phi^4(\bar{s}, f_c) \right]_{\Delta f}}{\left[Z(f_c) \right]_{\Delta f}^2} \tag{2.19}$$

$$\left| H_r^r(\bar{\xi}, f_c) \right|_{\Delta f}^2 \simeq (2\pi f_c)^4 \frac{\left[\phi^4(\bar{r}, f_c) \right]_{\Delta f}}{\left[Z(f_c) \right]_{\Delta f}^2} \tag{2.20}$$

Equations (2.18) through (2.20) contain three unknown quantities, namely

$$\left[Z(f_c) \right]_{\Delta f} , \quad \left[\phi^4(\bar{s}, f_c) \right]_{\Delta f} , \text{ and } \left[\phi^4(\bar{r}, f_c) \right]_{\Delta f} ,$$

which must be determined from the measured mobility functions

$$\left| H_r^s(\bar{\xi}, f_c) \right|_{\Delta f}^2 , \quad \left| H_s^s(\bar{\xi}, f_c) \right|_{\Delta f}^2 , \text{ and } \left| H_r^r(\bar{\xi}, f_c) \right|_{\Delta f}^2 .$$

One way to obtain the numerical values of the desired quantities, mentioned above, is by first assuming a trial value for $\left[Z(f_c) \right]_{\Delta f}$ and substituting it into equations (2.19) and (2.20) to obtain

$$\left[\phi^4(\bar{s}, f_c) \right]_{\Delta f} \quad \text{and} \quad \left[\phi^4(\bar{r}, f_c) \right]_{\Delta f} ;$$

then using equation (2.18) to check the computed value of $\left[Z(f_c) \right]_{\Delta f}$. If these two quantities do not agree numerically, the computed $\left[Z(f_c) \right]_{\Delta f}$ should be used in performing the same mathematical routine for the next trial. This iteration process will continue until a close agreement has been reached between trial and computed $\left[Z(f_c) \right]_{\Delta f}$. A simple computer routine could be written to perform such a task.

The above mathematical derivation shows that the point and transfer mechanical mobility measurements could be used to obtain frequency-average mode shapes and

modal impedance, which, as will be shown in the next section, play an important role in determining the joint acceptance function of a structure subjected to acoustic excitations.

2.5 Responses of a Linear Elastic Structure to Acoustic Excitations

Acceleration responses of a linear elastic structure to acoustic excitations could be expressed by the following equations [21] :

$$\Phi_{\ddot{\xi}}(\bar{r}, \omega) = \sum_m \sum_n \frac{\phi_m(\bar{r})\, \phi_n(\bar{r}) \cdot A^2}{Z_m(\omega)\, Z_n^*(\omega)} \Phi_{p_o}(\omega)\, J_{mn}^2(\omega) \qquad (2.21)$$

where

$\Phi_{\ddot{\xi}}(\bar{r}, \omega)$ = Power spectral density of acceleration at point $\bar{r}$

$\Phi_{p_o}(\omega)$ = Power spectral density of reference sound pressure which is assumed to be constant over the surface of a structure

A = surface area

$Z_m(i\omega)$ = modal impedance defined by equation (2.7)

$Z_n^*(i\omega)$ = complex conjugate of $Z_n(i\omega)$

$J_{mn}^2(\omega)$ = joint acceptance function of the mn-th mode

$$= \int_S \int_{S'} \frac{\phi_m(\bar{s})\, \phi_n(\bar{s}')}{A^2} \frac{\Phi_p(\bar{s}, \bar{s}', \omega)}{\Phi_{p_o}(\omega)}\, d\bar{s}\, d\bar{s}' \qquad (2.22)$$

$d\bar{s}, d\bar{s}'$ = infinitesimal area vectors

$\Phi_p(\bar{s}, \bar{s}', \omega)$ = cross-power spectral density of the sound pressure field.

Equation (2.21) could be written as

$$\frac{\Phi_{\ddot{\xi}}(\bar{r}, \omega)}{\Phi_{p_o}(\omega)} = \omega^4 \sum_m \sum_n \frac{\phi_m(\bar{r})\, \phi_n(\bar{r})\, A^2}{Z_m(\omega)\, Z_n^*(\omega)}\, J_{mn}^2(\omega) \qquad (2.23)$$

Equation (2.23) represents essentially the square of the modulus of the acceleration mobility function at point $\bar{r}$ to acoustic excitations. This acoustic mobility function, $\alpha_{\ddot{\xi}}(\bar{r}, \omega)$, can be written as:

$$\left|\alpha_{\ddot{\xi}}(\bar{r}, \omega)\right|^2 = \omega^4 \sum_m \sum_n \frac{\phi_m(\bar{r})\, \phi_n(\bar{r}) \cdot A^2}{Z_m(\omega)\, Z_n^*(\omega)} J_{mn}^2(\omega) \qquad (2.24)$$

Assume that the damping is small so that the cross-product terms can be neglected, equation (2.24) can be expressed by:

$$\left|\alpha_{\ddot{\xi}}(\bar{r}, \omega)\right|^2 = \omega^4 \sum_m \frac{\phi_m^2(\bar{r}) \cdot A^2}{\left|Z_m(\omega)\right|^2} J_{mm}^2(\omega) \qquad (2.25)$$

From equation (2.13), the frequency-average expression for equation (2.25) is

$$\left|\alpha_{\ddot{\xi}}(\bar{r}, f_c)\right|_{\Delta f}^2 = (2\pi f_c)^4 \frac{\left[\phi^2(\bar{r}, f_c)\right]_{\Delta f} \cdot A^2}{\left|Z(f_c)\right|_{\Delta f}^2} \left[J^2(f_c)\right]_{\Delta f} \qquad (2.26)$$

Then the joint acceptance function, $\left[J^2(f_c)\right]_{\Delta f}$, could be determined by:

$$\left[J^2(f_c)\right]_{\Delta f} = \frac{\left|\alpha_{\ddot{\xi}}(\bar{r}, f_c)\right|_{\Delta f}^2 \cdot \left|Z(f_c)\right|_{\Delta f}^2}{(2\pi f_c)^4 \left[\phi^2(\bar{r}, f_c)\right]_{\Delta f} \cdot A^2} \qquad (2.27)$$

or

$$\left[J^2(f_c)\right]_{\Delta f} = \frac{\left|\alpha_{\ddot{\xi}}(\bar{r}, f_c)\right|_{\Delta f}^2}{\left|H_r^{\bar{r}}(\bar{\xi}, f_c)\right|_{\Delta f}^2} \cdot \frac{\left[\phi^2(\bar{r}, f_c)\right]_{\Delta f}}{A^2}$$

The quantity $\left|\alpha_{\ddot{\xi}}(\bar{r}, f_c)\right|_{\Delta f}^2$ could be determined directly from acoustic-response

experimental data, whereas $\left[\phi^2(\vec{r}, f_c)\right]_{\Delta f}$ and $\left[\left|Z(f_c)\right|^2\right]_{\Delta f}$ could be computed from mechanical impedance measurement data. Thus the joint acceptance function, $\left[J^2(f_c)\right]_{\Delta f}$, could be determined from either equations (2.27) or (2.28). Once the joint acceptance function has been determined, the acoustic mobility function at any other point, say $\vec{s}$, on the structure is obtained simply by replacing $\left[\phi^2(\vec{r}, f_c)\right]_{\Delta f}$ in equation (2.26) with $\left[\phi^2(\vec{s}, f_c)\right]_{\Delta f}$ which has been computed through mobility measurement data. Consequently the response power spectral density at $\vec{s}$ to random acoustic excitations could be determined by [21]:

$$\Phi_{\dot{\xi}}(\vec{s}, f_c) = \left|\alpha_{\dot{\xi}}(\vec{s}, f_c)\right|^2_{\Delta f} \quad \Phi_p(f_c) \tag{2.29}$$

where

$\Phi_p(f_c)$ = Power spectral density of reference acoustic pressure which is assumed to be constant over the structural surface.

The mechanical impedance (or mobility) concepts, in predicting structural responses to acoustic excitations, as discussed in this section, can be presented schematically by a flow chart, as shown in Figure 2.3, in which the required measurements include impedance (or mobility) measurements, sinesweep acoustic and response measurements, and random acoustic measurements. The mechanical mobility data together with sinesweep acoustic data would determine the following quantities (in a frequency-average sense):

- mode shapes - $\left[\phi^2(\vec{s}, f_c)\right]_{\Delta f}$ .....
- modal impedance - $\left|Z(f_c)\right|^2_{\Delta f}$
- acoustic mobility function - $\left|\alpha_{\dot{\xi}}(\vec{s}, f_c)\right|^2_{\Delta f}$, ...

These quantities, in turn, determine acoustic mobility functions at other measurement points on the surface. The random acoustic power spectral density, determined from random acoustic excitation, multiplied by the acoustic mobility function of a measurement point would yield the power spectral density of response at that point.

The technique presented in this section could be easily adopted for an on-line data acquisition system. Such a system could provide rapid answers to the vibro-acoustic response problems once it receives measurement data of structures and acoustic pressure fields. This technique is, however, not limited to the application of acoustic excitation fields. The same principle and equations could be applied to other loading conditions, such as aerodynamic, hydrodynamic fields, etc., with equal effectiveness.

3.0 EXPERIMENTAL PROGRAM

The objectives of this experimental program are to study the applicability of point impedance (or mobility) measurements in predicting dynamic responses of structures to acoustic excitations and to verify response equations derived in the previous sections.

Three types of rectangular panels with a typical lateral dimension of 24.48" x 16.80" were tested in the parallel incident direction of a Wyle Acoustic Test Facility, as shown in Figure 3.1. These panels could be classified as

a) the rigid panel (Figure 3.2);

b) the stiffened panel (Figure 3.3); and

c) the plain panel (Figure 3.4),

and subjected to four types of tests as tabulated in Table 1.

The analog response signals and forcing signals were digitalized by Wyle's on-line CDC 3300 digital data acquisition system and were stored on magnetic tapes for subsequent analyses. Description of test fixtures and panels, instrumentations, data acquisition systems and test procedures are presented in the following sections.

3.1 Description of Test Fixture and Panels

The test fixture consists of a rectangular concrete block, as shown in Figure 3.5, with a dimension of 76-1/8" x 52-7/8" x 12", and a 24.48" x 16.80" opening located at its center. This opening was fitted with an aluminum frame, as shown in Figures 3.5 and 3.6, which was used to fasten test panels to the fixture. Detailed information on the test fixture could also be found on Wyle Drawing Numbers E19636 and E19637.

The rigid panel, as shown in Figure 3.2 is made of 1-1/2" aluminum plate with a layer of 1/2" Vibrodamp damping compound as backing. A rectangular aluminum frame fabricated from aluminum angle (L1 x 1 x 1/4) was bolted to the rigid frame to serve as a mounting bracket. Three 1/4" and three 1/2" holes are provided in the panel for installing microphones.

The stiffened panel, as shown in Figure 3.3, was machined from a piece of solid aluminum plate 0.96" thick. The use of an integral stiffened section is necessary in order to eliminate any possible variation in impedance characteristics due to slippage between stiffeners and the panel. This might happen if other types of connections (such as rivets or bolts and nuts) were used. The dimension of the stiffener is 0.928" x 0.096".

The plain panel is made of an aluminum plate with a thickness of 0.365". The thickness of this plate was established so as to provide the same amount of section modulus as that of the stiffened panel which has an average value of 4.03×10^{-3} in^4/in. Three strips of 3M - damping tape were applied to the back of the panel to increase damping. Details of the unstiffened panel are shown in Figure 3.4.

3.2 Instrumentation and Data Acquisition System

Transducers used in performing tests on each panel have been tabulated in Table II. The model designation of listed instruments are described as follows:

a) Air Modulator - WAS 3000

b) Impedance Head - Wilcoxson Z-602

c) Shaker - Wilcoxson F-1

d) Accelerometers - Endevco Microminiature Type 2226

e) Microphones - B and K.

The signal transducers used in the rigid panel tests included seven microphones (M1 - M7) as shown in Figure 3.2, with M7 microphone located approximately 2" from the leading edge of the panel to serve as a control microphone. Microphones M1 through M6 were mounted on the rigid panel with diaphragms set flush to the panel surface by six specially designed microphone holders. Seven accelerometers (A1 - A7), as shown in Figures 3.3 and 3.7, were used in testing the stiffened panel while six accelerometers (A1 - A6) were used in testing the plain panel. Each accelerometer weighs 2.75 grams. The locations of these accelerometers were identical with those of microphones (M1 - M6) for the rigid panel but with A7 accelerometer located at the center of the stiffened panel.

In testing the stiffened and the plain panel, three rows of elastic chords were installed vertically inside the test section, and six microphones were tied to these chords at the approximate locations of corresponding accelerometers (A1 - A6) with diaphragms positioned very close to the test panel.

The force and response signals were monitored by Wyle Acoustic Test control system shown in Figure 3.8, and were transmitted through charge and buffer amplifiers, respectively, to Wyle's A/D data acquisition system to be processed and stored on magnetic tapes for later data reduction use. Schematic diagrams showing the complete data acquisition system are presented in Figures 3.9 and 3.10.

3.3 Test Procedures

The sweep rate of Wyle's A/D data acquisition system used in acquiring impedance measurements and sinesweep acoustic tests of a structure depends on the dynamic

magnification factor, Q, of the test structure. Therefore, Q-measurements were performed first on the stiffened and the plain panels to determine proper sweep rates for testing each panel.

To obtain these Q-measurements, several trail runs were performed with the test panel placed in the test section and excited it with sinesweep acoustic excitation (130 dB at 1/2 octave/min.). An accelerometer signal was monitored to locate resonant frequencies of the test panel. After a suitable peak amplitude was chosen, the resonant frequency, f_o, was recorded; then by controlling the frequency modulator, the upper and lower frequency limits at which the amplitudes of response were 3 dB lower than the peak, were obtained.

The Q-value of the test panel was determined by equation (3.1)

$$Q = \frac{f_o}{f_u - f_\ell} \tag{3.1}$$

where

f_o = resonant frequency

f_u = upper frequency limit

f_ℓ = lower frequency limit.

Typical test curves are shown in Figures 3.11 and 3.12 for the stiffened and the plain panels, respectively. The approximate Q-values for these panels were:

$$Q_{stiffened} = 30$$

$$Q_{plain} = 60$$

Therefore, the sweep rate used in the latter tests were 1 octave/min. for the stiffened panel and 1/2 octave/min. for the plain panel.

Impedance measurements were made on the stiffened and the plain panels, respectively, before conducting acoustic tests. A Wilcoxson Z602 impedance head with a F-1 shaker was used to excite the test panel at designated locations. A total of eight point-excitations were made on the stiffened panel, and six point-excitations were made on the plain panel. Test numbers and other details for both panels are tabulated in Tables III and IV.

Acoustic tests were performed on all three panels. The rigid panel was used to measure the pressure correlation patterns as well as one-third octave random pressure spectra, of microphones M1 - M6 as shown in Figures 3.13 through 3.19, respectively. Total number of acoustic tests for test panels are described as follows:

a) One sinesweep and two random acoustic tests for rigid panel.

b) Two sinesweep and three random acoustic tests for the stiffened panels; and

c) One sinesweep and one random acoustic test for the plain panel.

Test numbers and other details for these tests were presented in Tables V, VII and VIII.

4.0 SUMMARY

The development of mechanical impedance measurement techniques to predict structural responses to acoustic excitations has been presented in this report. Tests were performed on three types of panels, namely, the rigid, the stiffened and the plain panels, so that comparisons between the predicted and the experimental responses could be made. Wyle A/D data acquisition system was utilized in all tests, and digitalized data tapes will be used to compute frequency - averaged joint acceptance functions and responses of these test panels in a later report.

REFERENCES

1. Smith, P.W. Jr. and Lyon, R.H., "Sound and Structural Vibration," NASA CR-160, March 1965.

2. Lyon, R.H., "Sound Radiation from a Beam Attached to a Plate," The Journal of the Acoustical Society of America, Vol. 34, No. 9, Part I, September 1962, pp. 1265-1268.

3. Maidanik, G., "Response of Ribbed Panels to Reverberant Acoustic Fields," The Journal of the Acoustical Society of America, Vol. 34, No. 6, June 1962, pp. 809-826.

4. Lyon, R.H. and Maidanik, G., "Power Flow between Linearly Coupled Oscillators," The Journal of the Acoustical Society of America, Vol. 34, No. 5, May 1962, pp. 623-639.

5. Powell, A., "On the Fatigue Failure of Structures due to Vibrations Excited by Random Pressure Fields," The Journal of the Acoustical Society of America, Vol. 30, No. 12, December 1958, pp. 1130-1135.

6. Powell, A., "On the Response of Structures to Random Pressures and to Jet Noise in Particular," Chapter 8, Random Vibration, Vol. 1, John Wiley and Sons, Inc., New York, 1958.

7. Powell, A., "On the Approximation to the "Infinite" Solution by the Method of Normal Modes for Random Vibrations," The Journal of the Acoustical Society of America, Vol. 30, No. 12, December 1958, pp. 1136-1139.

8. Bozich, D.J., "Spatial Correlation in Acoustic-Structural Coupling," The Journal of the Acoustical Society of America, Vol. 36, No. 1, January 1964, pp. 52-58.

9. Wenzel, A., "Joint Acceptance Functions for Cylinders," Wyle Laboratories Research Staff Report WR 67-9, June 1967.

10. White, R.W., "Predicted Vibration Responses of Apollo Structure and Effects of Pressure Correlation Length on Response," Wyle Laboratories - Research Staff Report WR 67-4, March 1967.

11. Heckl, M.A. Lyon, R.H. Maidanik, G. and Ungar, E.E., "New Approach to Flight Vehicle Structural Vibration Analysis and Control," AD 290 798.

12. Lyon, R.H., "An Energy Method for Prediction of Noise and Vibration Transmission," Shock, Vibration and Associated Environment, Bulletin No. 33, Part II, February 1964, pp. 13-25.

13. Heckl, M., "Measurements of Absorption Coefficients on Plates," The Journal of the Acoustical Society of America, Vol. 34, No. 6, June 1962, pp. 803-808.

14. Dyer, I., "Estimation of Sound-Induced Missile Vibration," Chapter 9, Random Vibration, Vol. 1, John Wiley and Sons, Inc., New York, 1958.

15. Dyer, I., "Response of Space Vehicle Structures to Rocket Engine Noise," Chapter 7, Random Vibration, Vol. 2, John Wiley and Sons, Inc., New York, 1963.

16. Franken, P.A. and Lyon, R.H., "Estimation of Sound-Induced Vibrations by Energy Methods, with Applications to the Titan Missile," Shock, Vibration and Associated Environments, Bulletin No. 31, Part II, April 1963, pp. 12-16.

17. Jewell, R.E., "A Technique for Predicting Localized Vibration Environments In Rocket Vehicles and Space Craft," Shock, Vibration and Associated Environments, Bulletin No. 33, Part II, April 1963, pp. 26-33.

18. Kao, G. et al., "Summary Report on the Study of Impedance Evaluation Techniques," Research and Analysis Section Technical Memorandum No. 185, Northrop Space Laboratories, June 1966.

19. White, R.W. et al., "Empirical Correlation of Excitation Environment and Structural Parameters with Flight Vehicle Vibration Response," AD 610 482, December 1964.

20. Bozich, D.J. and Sutherland, L.C., "Mechanical and Acoustic Mobility of Saturn Instrument Unit - A Theoretical and Experimental Study Utilizing Digital Data Reduction Techniques," Wyle Laboratories Research Staff Report, WR 66-38, July 1966.

21. Robson, J.D., "An Introduction to Random Vibration," Elsevier Publishing Co., New York, 1964.

TABLE I

CLASSIFICATIONS OF TESTS

Type of Panel	TEST CLASSIFICATION			
	Evaluation of Dynamic Magnification Factor Q	Impedance Measurement	Acoustic Excitation	
			Sinesweep	Random
Rigid Panel	No	No	Yes	Yes
Stiffened Panel	Yes	Yes	Yes	Yes
Plain Panel	Yes	Yes	Yes	Yes

TABLE II

TRANSDUCERS USED IN TESTS

Instrument	Rigid Panel	Stiffened Panel	Plain Panel
Air Modulator	Yes	Yes	Yes
Impedance Head and Shaker	No	Yes	Yes
Accelerometers	No	Yes	Yes
Microphones	Yes	Yes	Yes

TABLE III

IMPEDANCE MEASUREMENT OF STIFFENED PANEL

Date	Test No.	Driving Pt.	Sweep Rate (Octave/min.)	Frequency Range (Hz.)	Remarks
2/28/67	2093	A1	1	40 - 1280	
2/28/67	2094	A2			
2/28/67	2095	A3			
2/28/67	2096	A4			
2/28/67	2097	A5			
2/28/67	2098	A6			
2/28/67	2099	A7			Observation windows left open
2/28/67	2100	A2	1	40 - 1280	Observation window left open

TABLE IV

IMPEDANCE MEASUREMENT OF PLAIN PANEL

Date	Test No.	Driving Pt.	Sweep Rate (Octave/min.)	Frequency Range (Hz.)	Remarks
3/7/67	2104	1	1/2	100 - 1200	
3/7/67	2105	2			
3/7/67	2106	3			
3/7/67	2107	4			
3/7/67	2108	5			
3/7/67	2109	6	1/2	100 - 1200	

TABLE V

ACOUSTIC TESTS OF RIGID PANEL

Date	Test No.	Type of Excitation	S.P.L.	Sweep Rate (Octave/min.)	Frequency Range (Hz.)
2/24/67	2090	Acoustic Sinesweep	130 dB	1/2	40 - 1100
2/24/67	2091	Acoustic Random	130 dB	-	
2/24/67	2092	Acoustic Random	130 dB	-	40 - 1100

TABLE VI

ACOUSTIC TESTS OF STIFFENED PANEL

Date	Test No.	Type of Excitation	S.P.L.	Sweep Rate (Octave/min.)	Frequency Range (Hz.)
3/1/67	2101	Sinesweep	130 dB	1.0	40 - 1280
3/1/67	2102	Random	130 dB	-	40 - 1280
3/1/67	2103	Random	130 dB	-	40 - 1280
3/8/67	2112	Sinesweep	120 dB	1.0	40 - 1280
3/8/67	2113	Random	120 dB	-	40 - 1280

TABLE VII

ACOUSTIC TESTS OF PLAIN PANEL

Date	Test No.	Type of Excitation	S.P.L.	Sweep Rate (Octave/min.)	Frequency Range (Hz.)
3/7/67	2110	Sinesweep	130 dB	1/2	100 - 1200
3/7/67	2111	Random	130 dB	-	100 - 1200

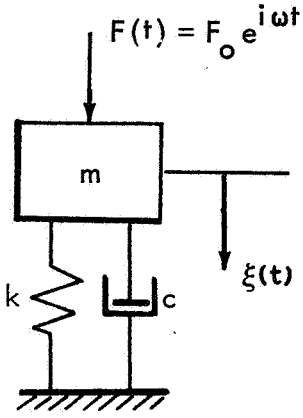

FIGURE 2.1 SINGLE DEGREE-OF-FREEDOM SYSTEM

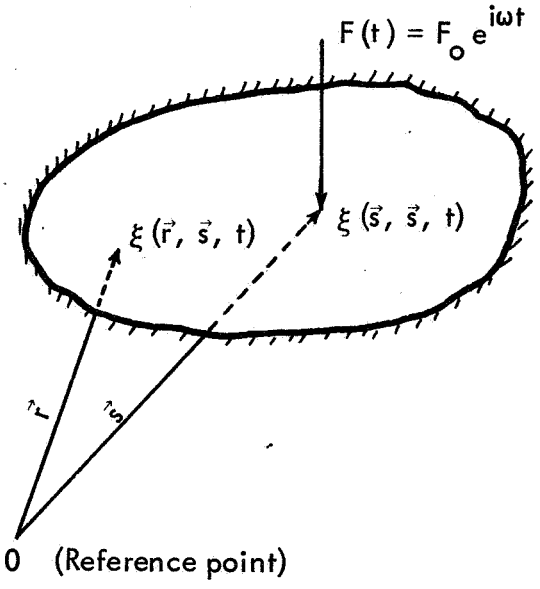

FIGURE 2.2 CONTINUOUS STRUCTURAL SYSTEM

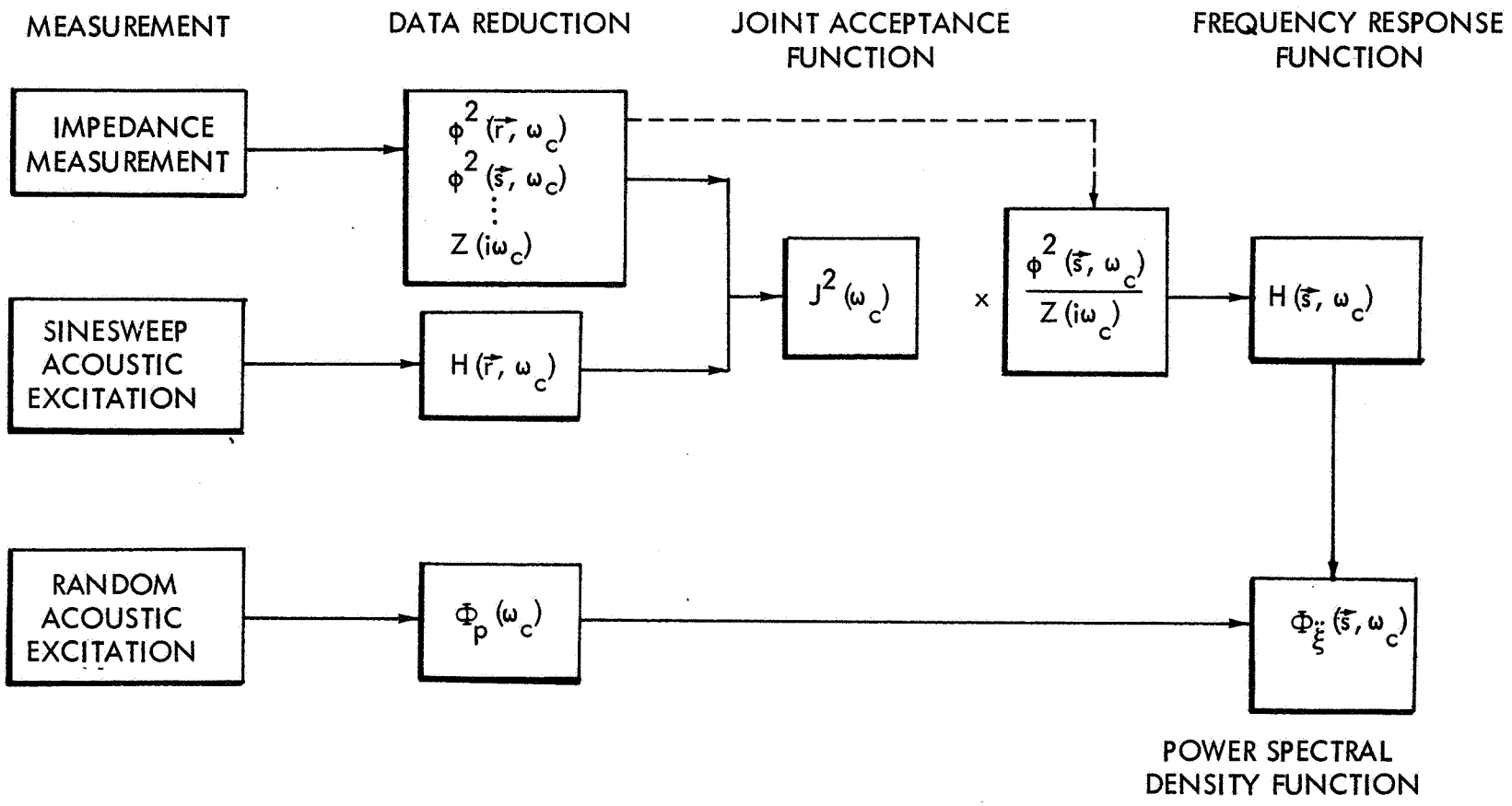

FIGURE 2.3 APPLICATION OF IMPEDANCE MEASUREMENT TECHNIQUE

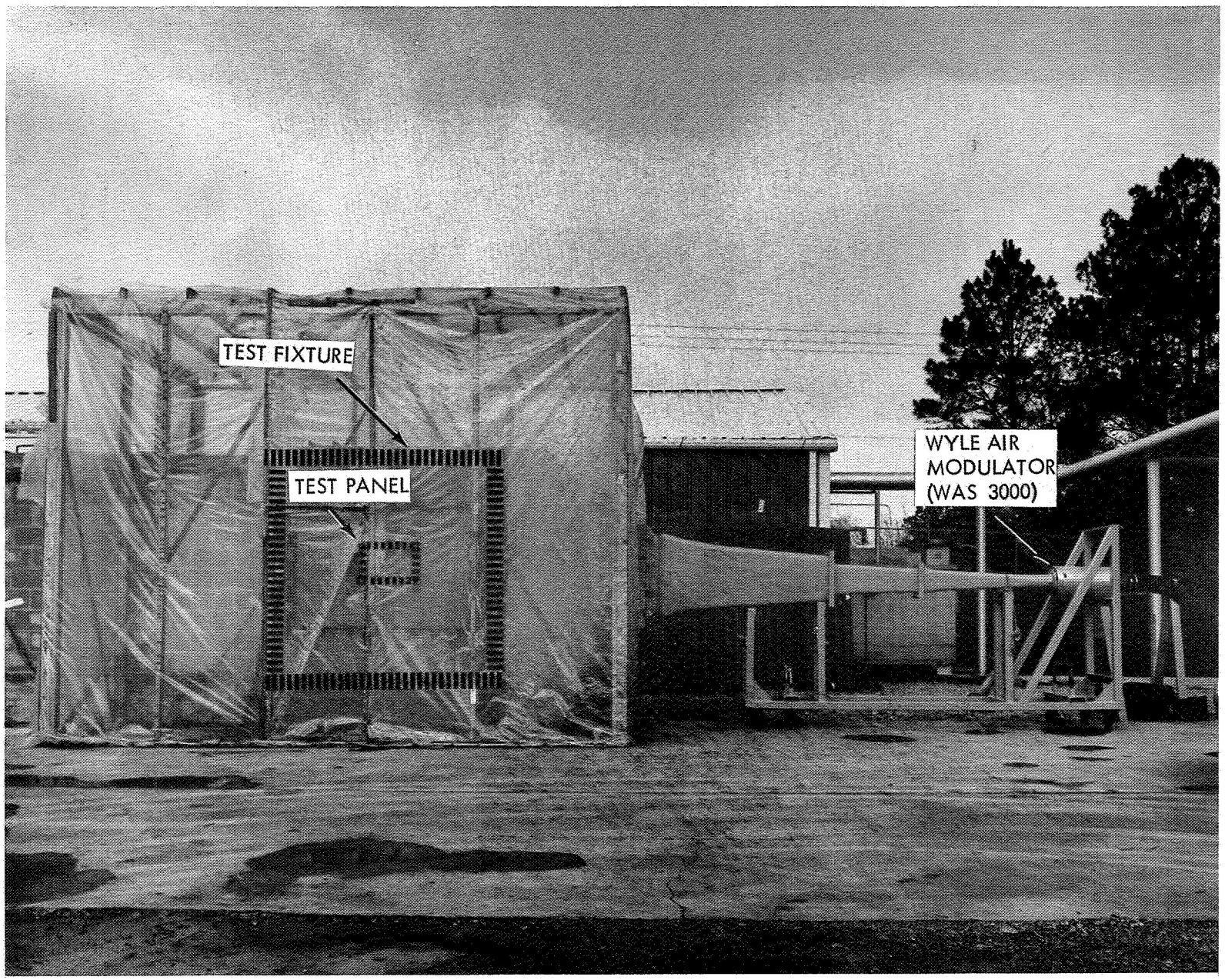

FIGURE 3.1 WYLE ACOUSTIC TEST FACILITY

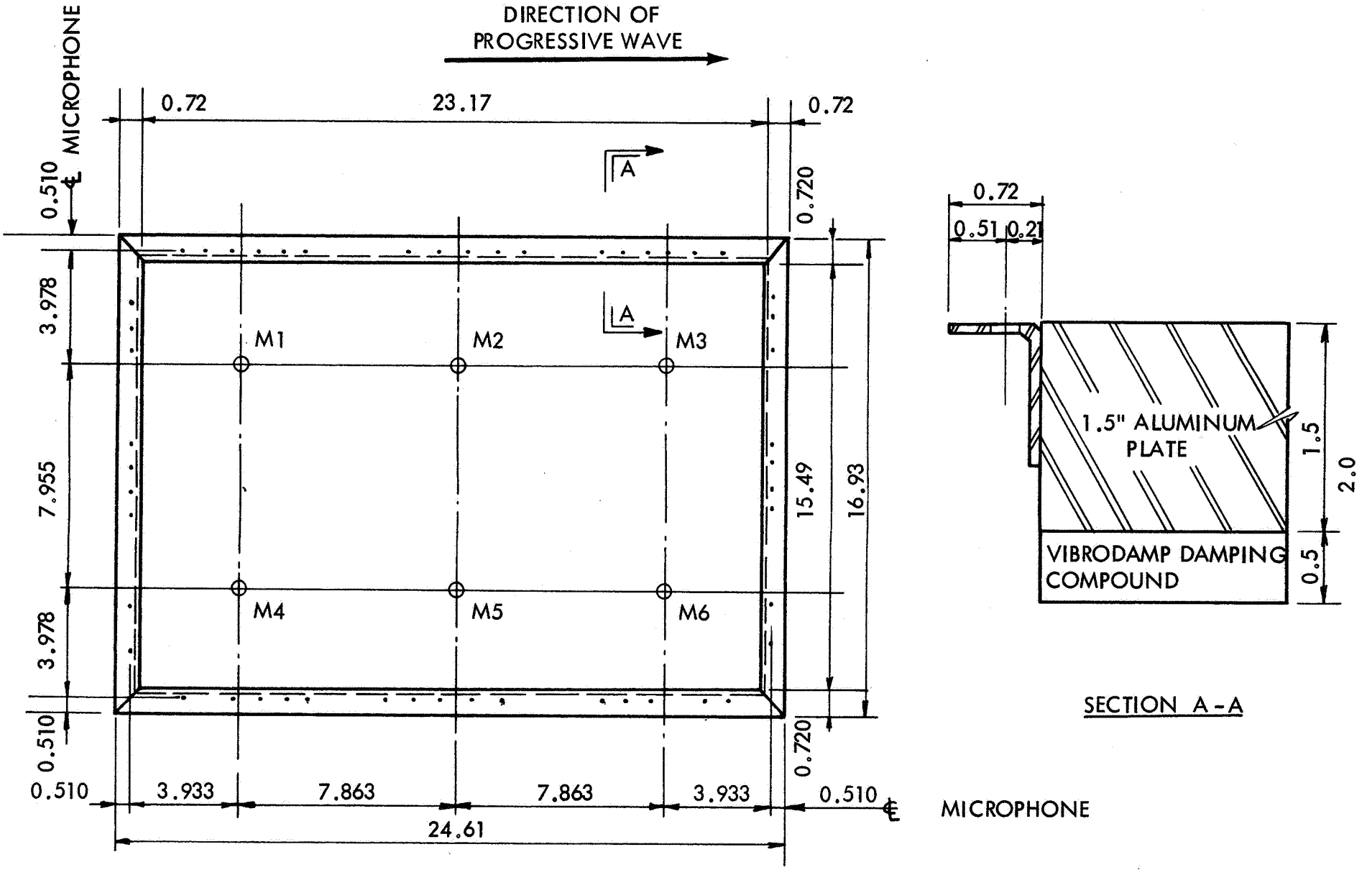

FIGURE 3.2 RIGID PANEL (UNIT = INCH)

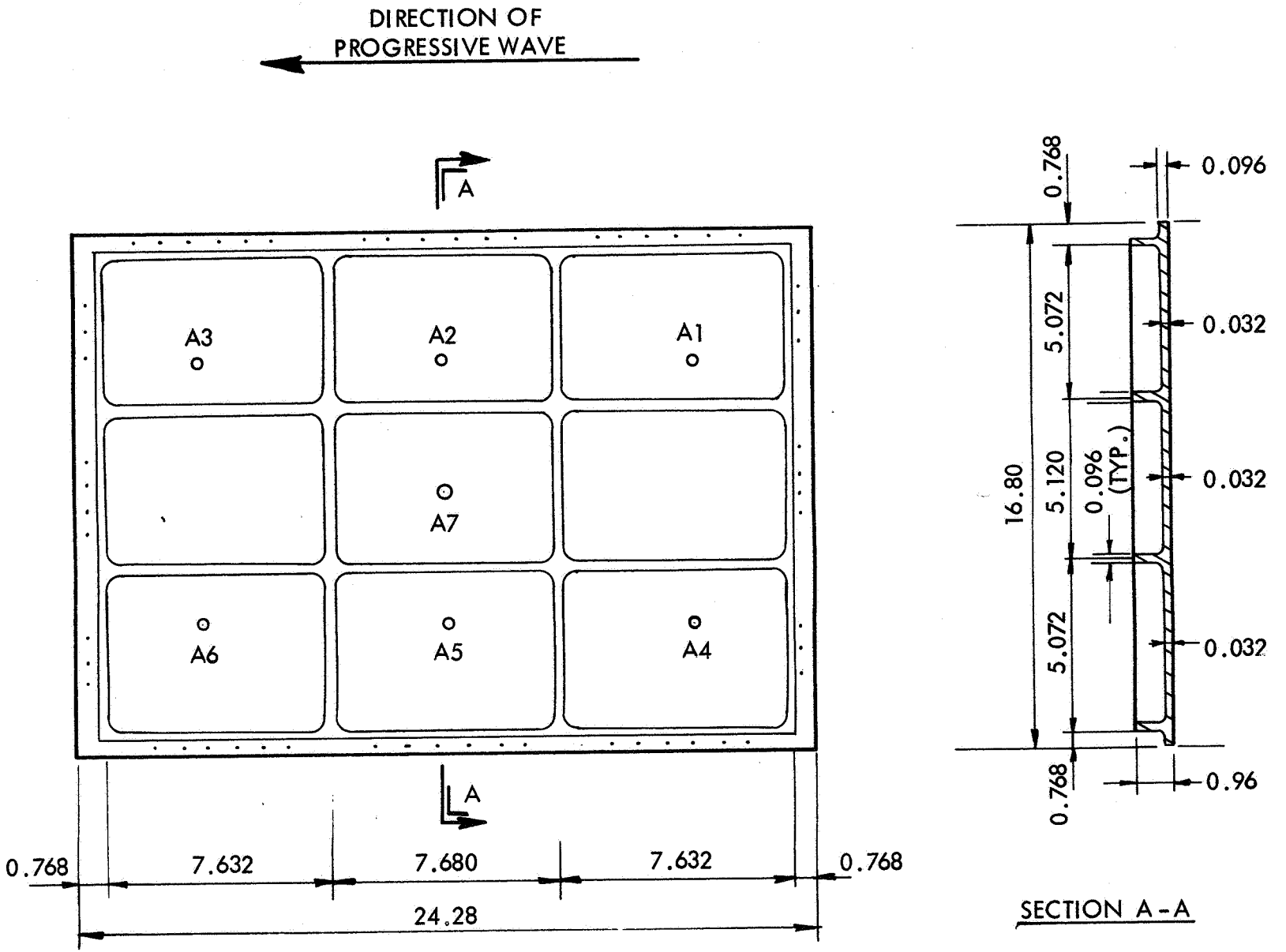

FIGURE 3.3 STIFFENED PANEL (UNIT = INCH)

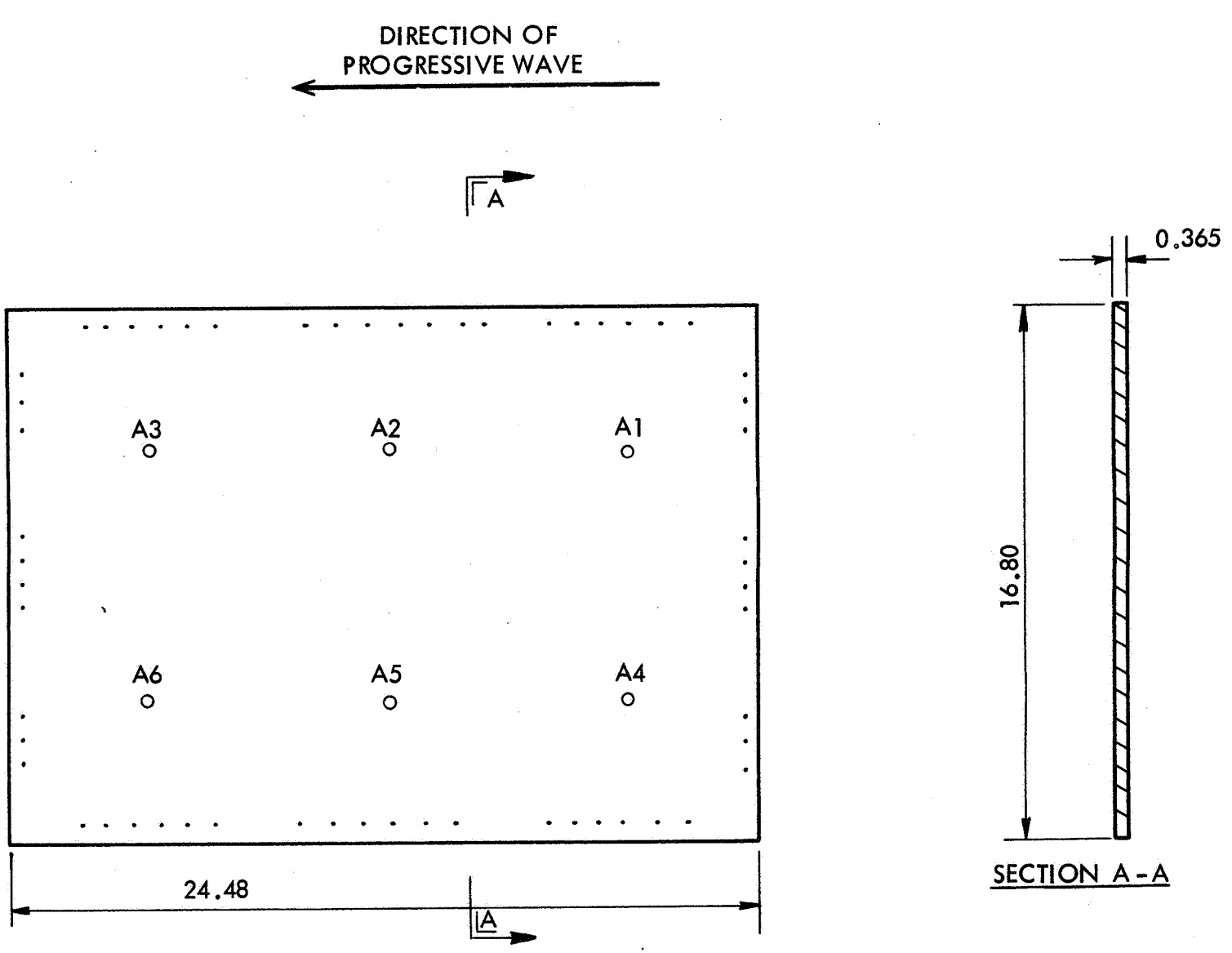

FIGURE 3.4 PLAIN PANEL (UNIT = INCH)

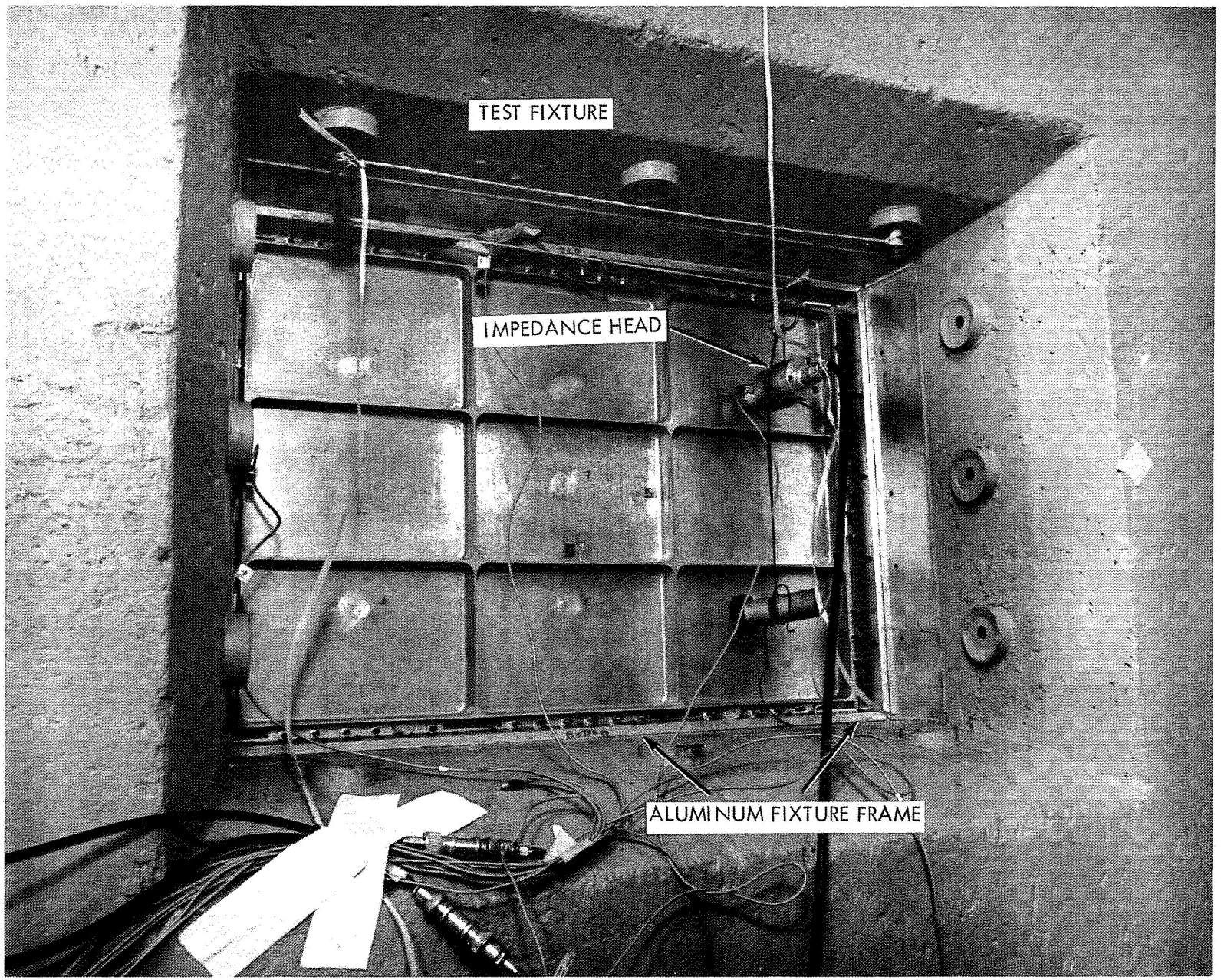

FIGURE 3.5 TEST FIXTURE

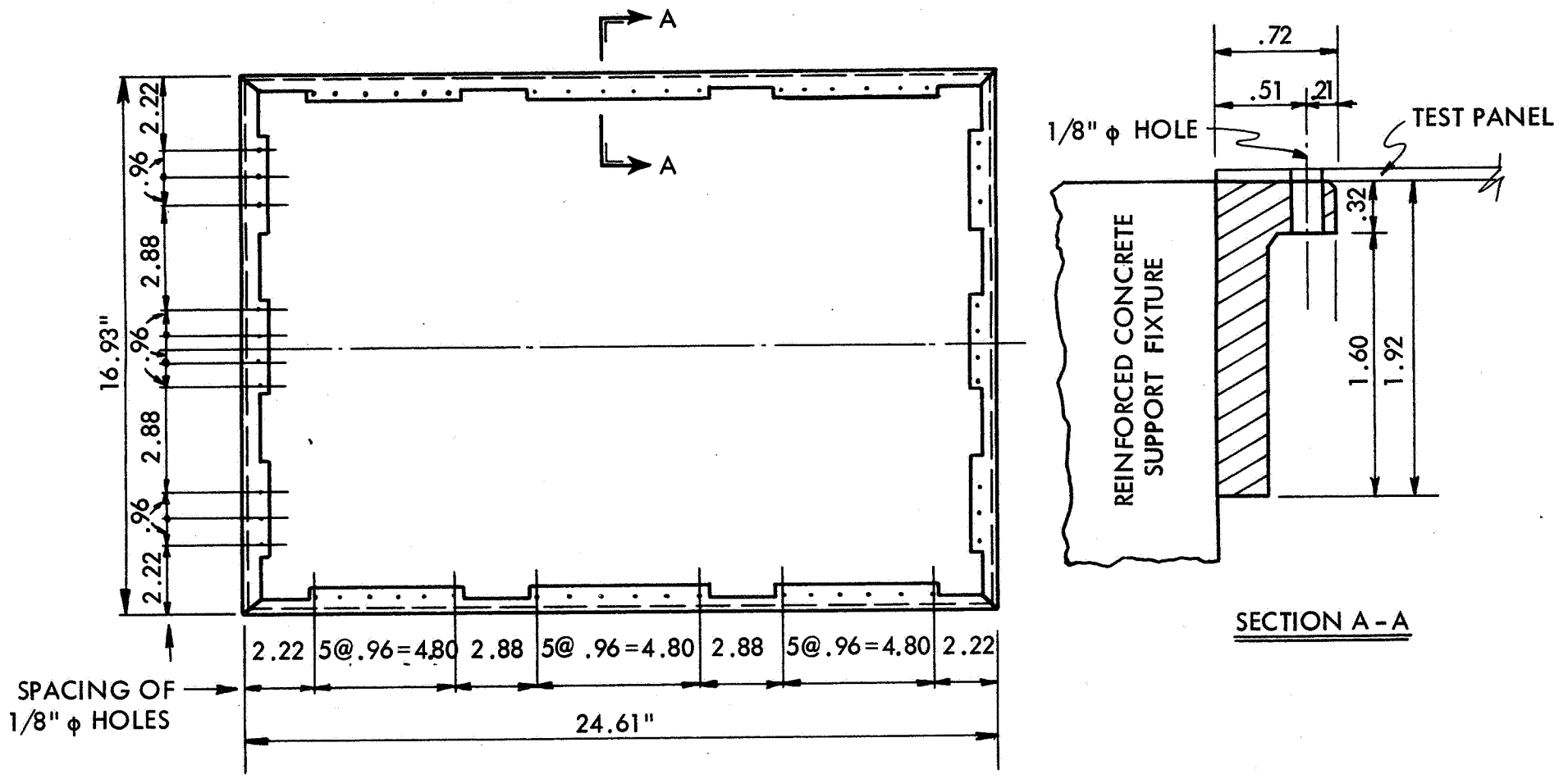

FIGURE 3.6 ALUMINUM FRAME FIXTURE

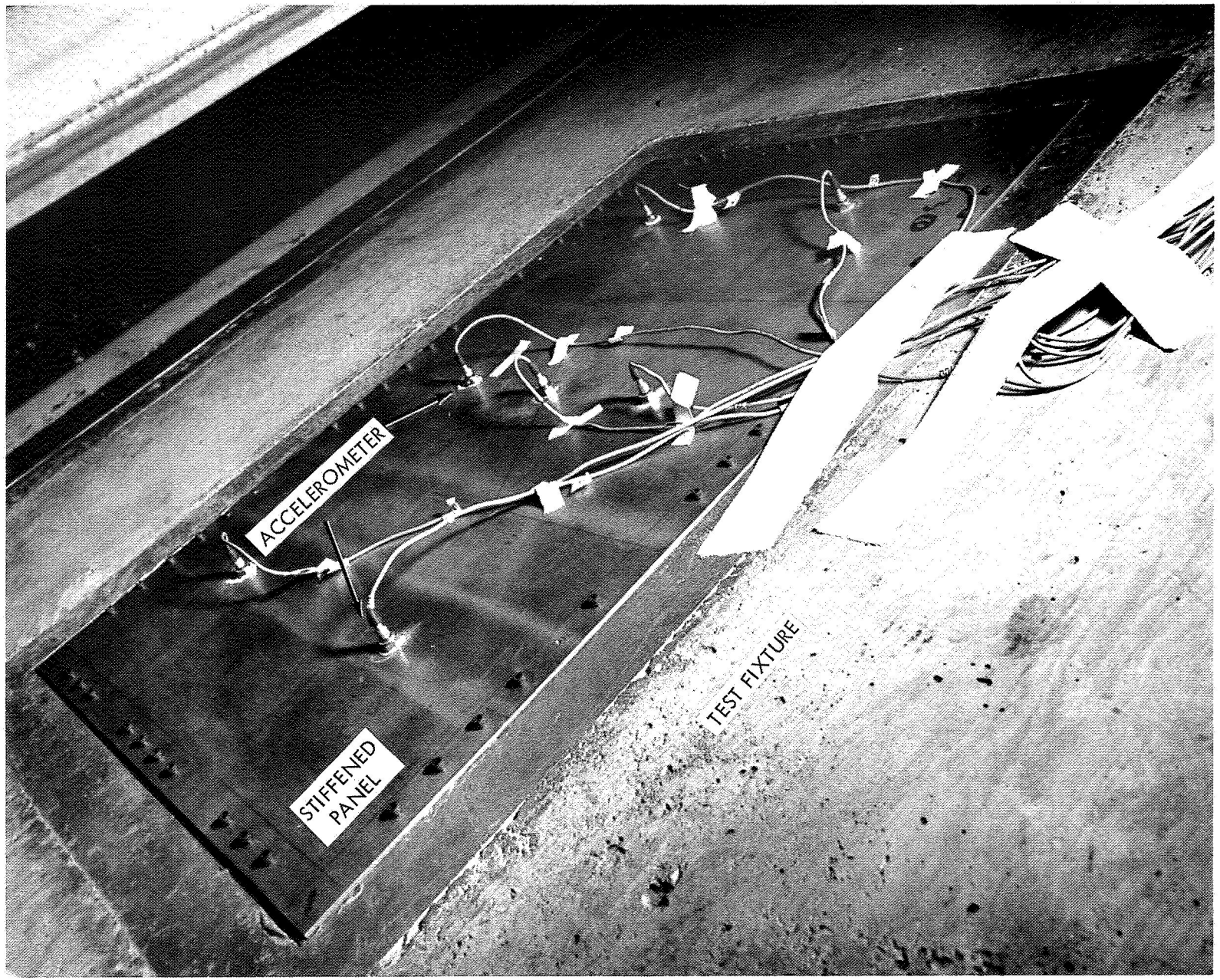

FIGURE 3.7 LOCATIONS OF ACCELEROMETERS OF THE STIFFENED PANEL

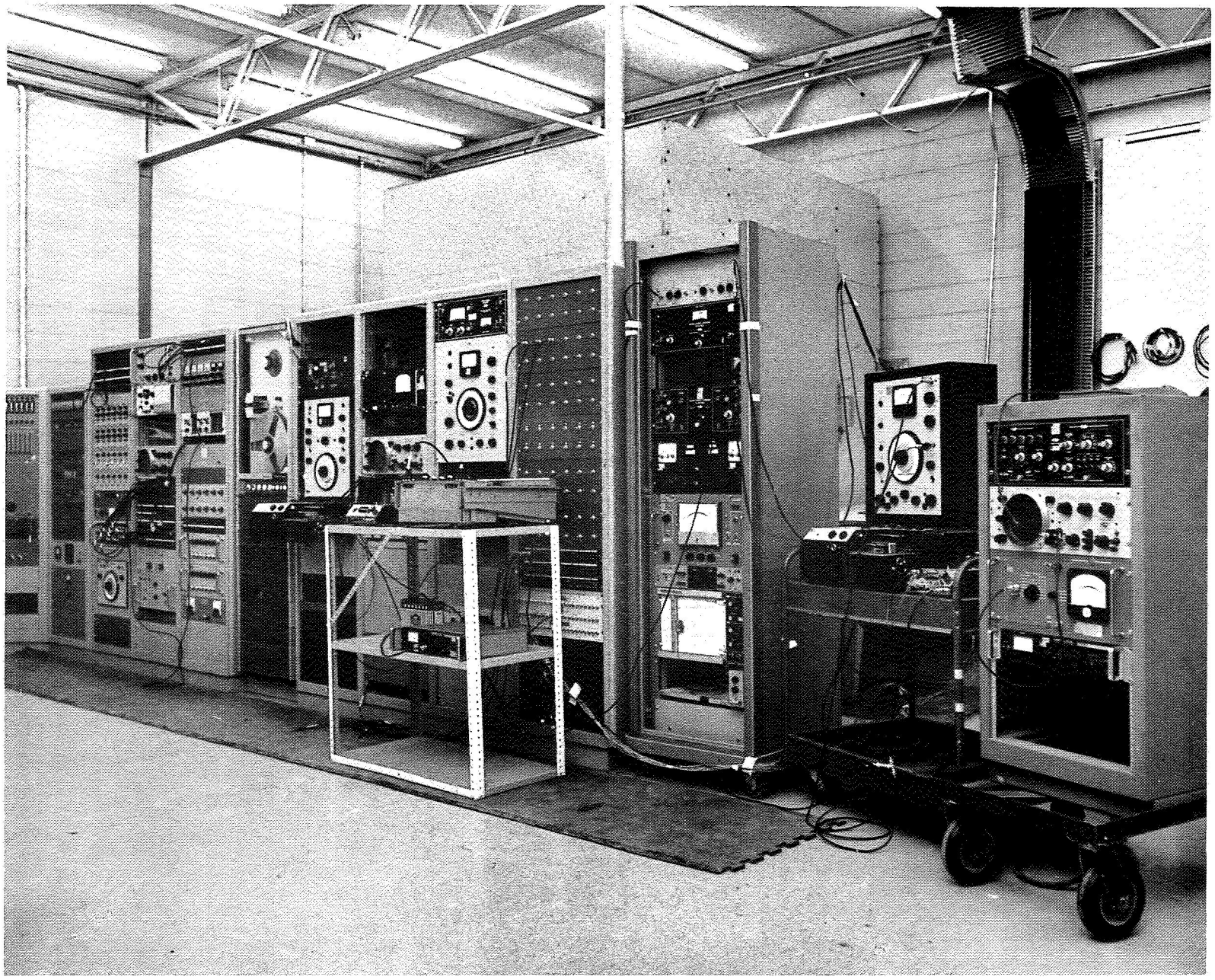

FIGURE 3.8 WYLE ACOUSTIC TEST CONTROL SYSTEM

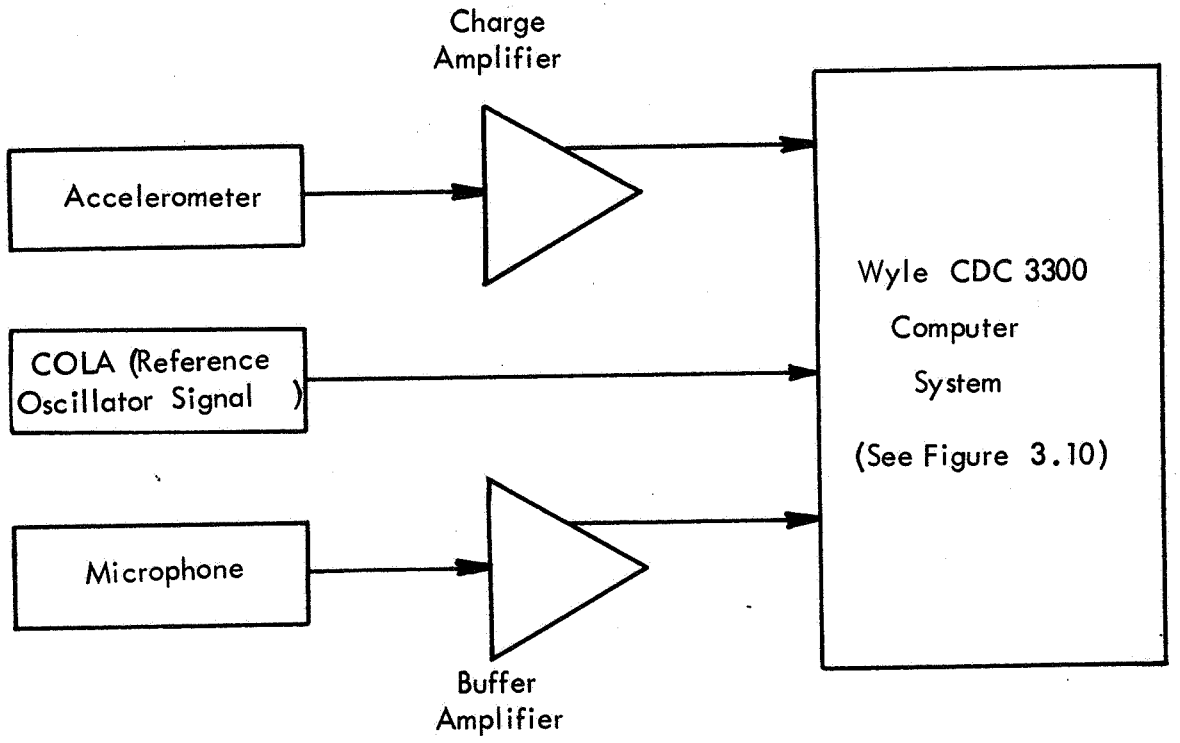

FIGURE 3.9 BLOCK DIAGRAM OF WYLE DATA ACQUISITION SYSTEM

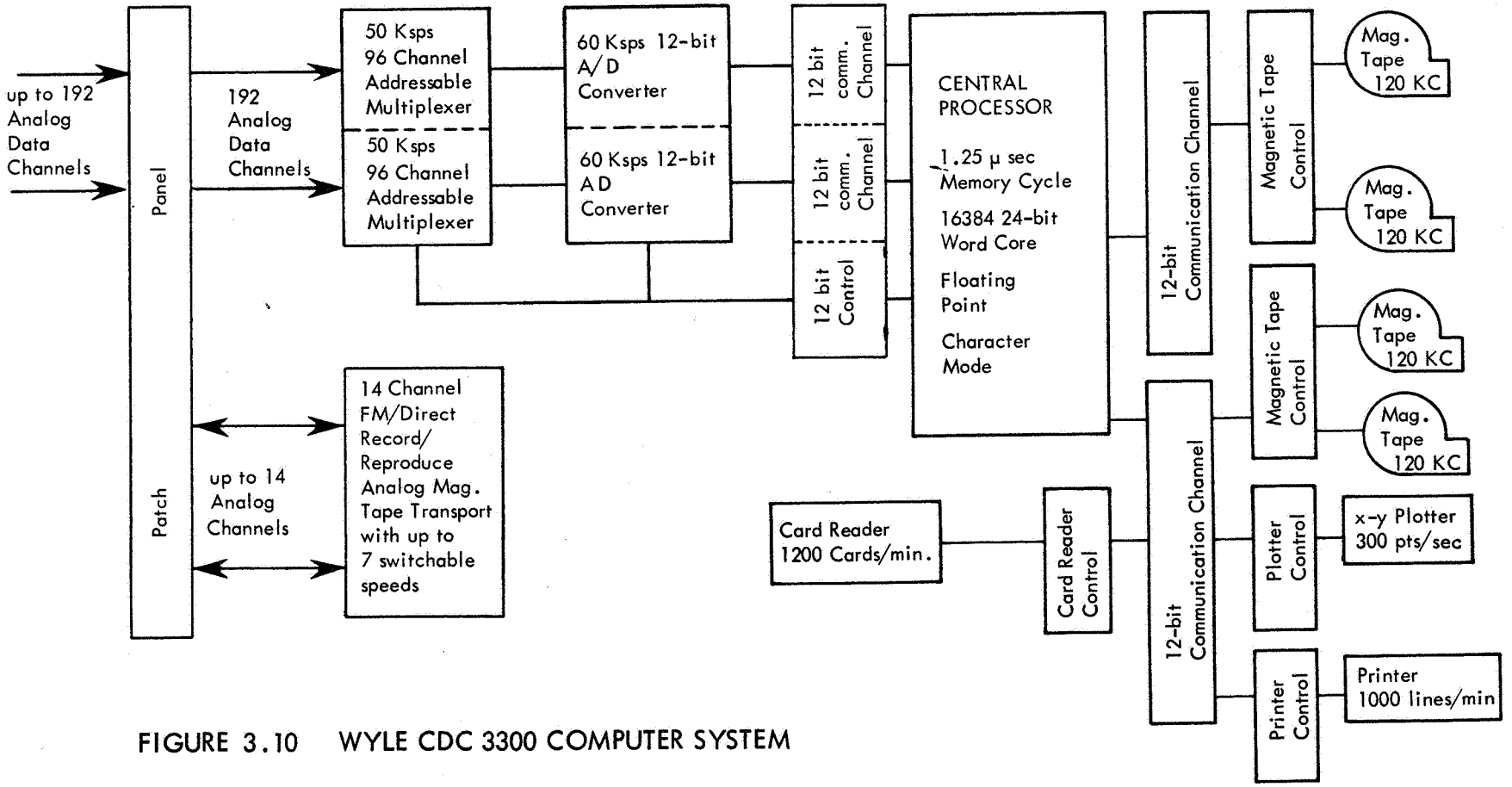

FIGURE 3.10 WYLE CDC 3300 COMPUTER SYSTEM

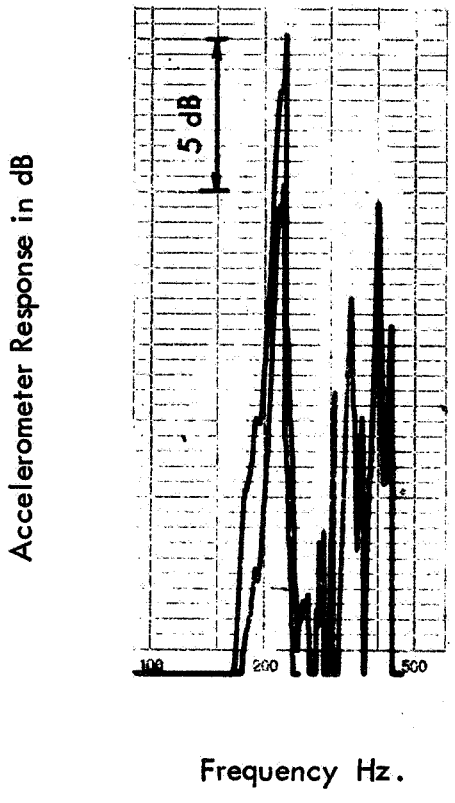

FIGURE 3.11 Q-MEASUREMENT OF STIFFENED PANEL
(Mean Sound Pressure Level = 130 dB)

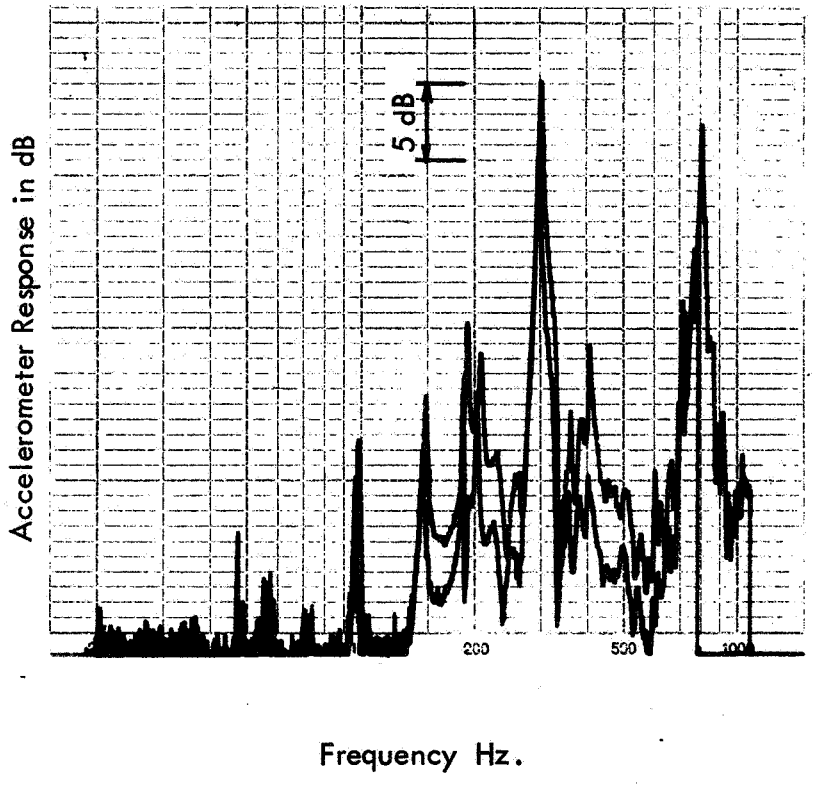

FIGURE 3.12 Q-MEASUREMENT OF PLAIN PANEL
(Mean Sound Pressure Level = 130 dB)

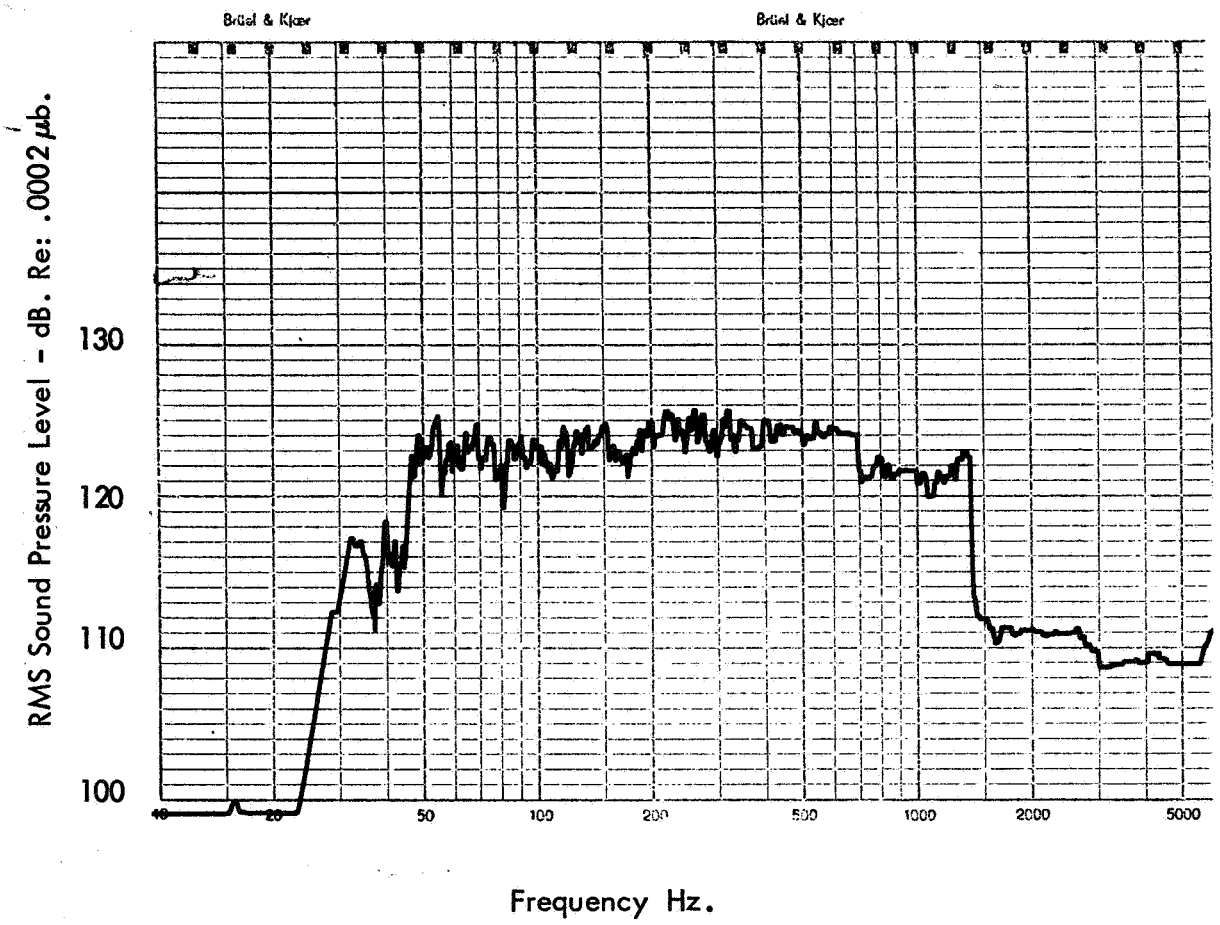

FIGURE 3.13 SOUND PRESSURE LEVEL SPECTRUM OF MICROPHONE M7

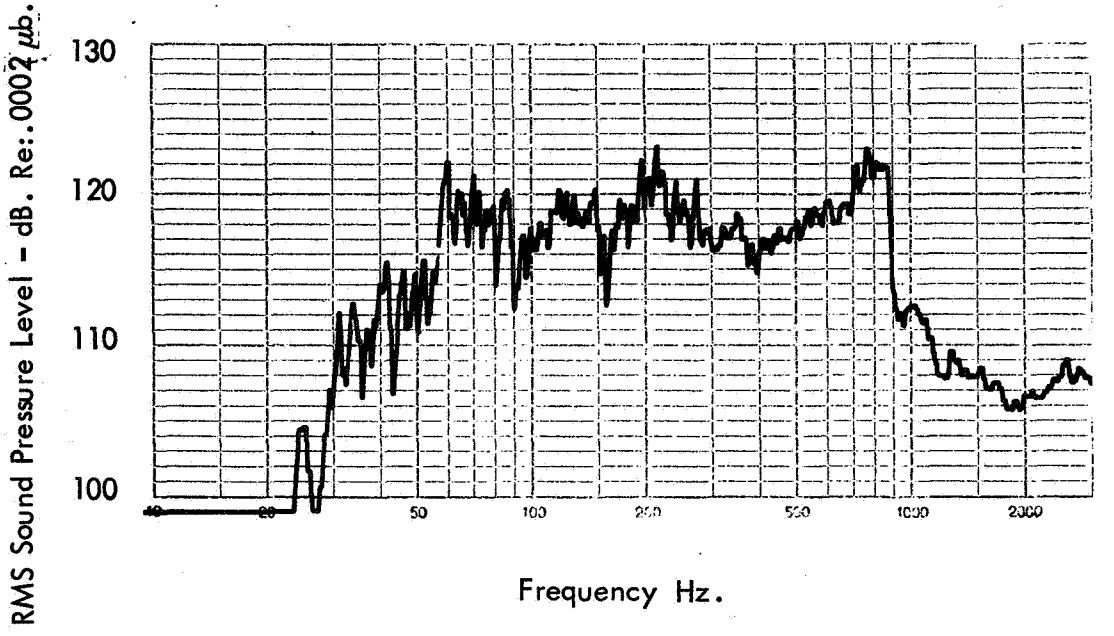

FIGURE 3.14 SOUND PRESSURE LEVEL SPECTRUM OF MICROPHONE M1

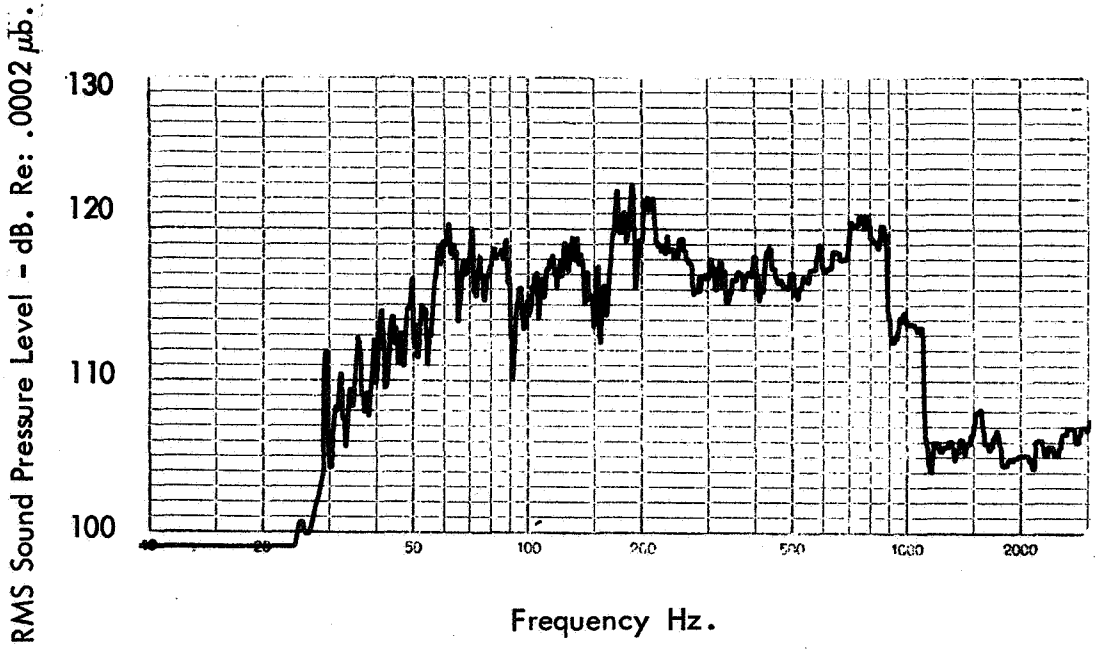

FIGURE 3.15 SOUND PRESSURE LEVEL SPECTRUM OF MICROPHONE M4

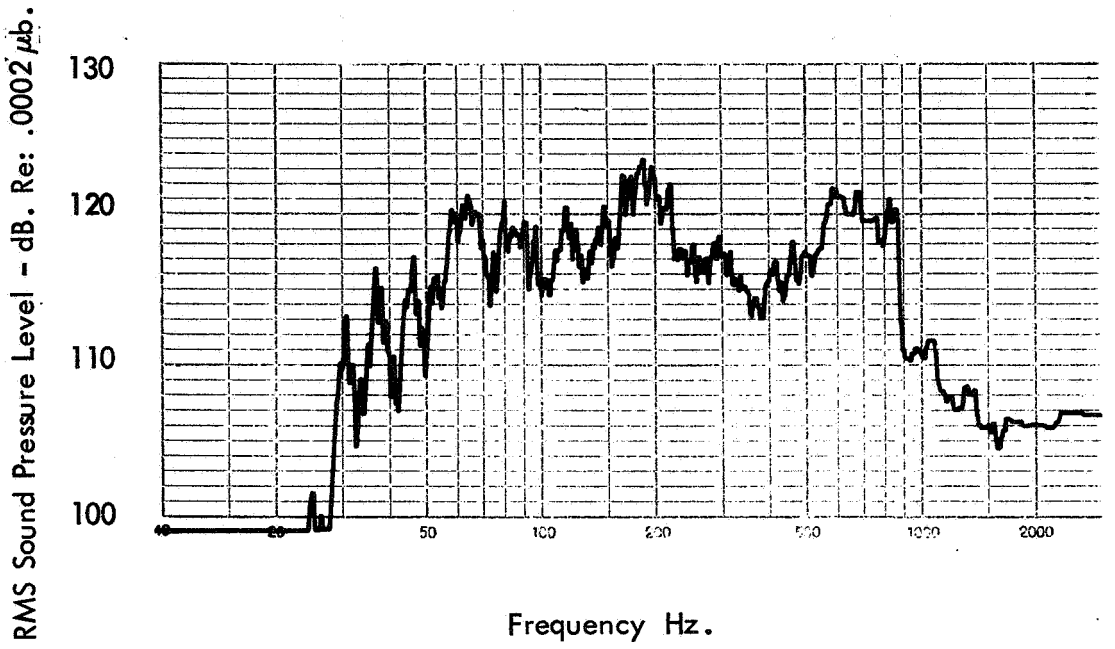

FIGURE 3.16 SOUND PRESSURE LEVEL SPECTRUM OF MICROPHONE M2

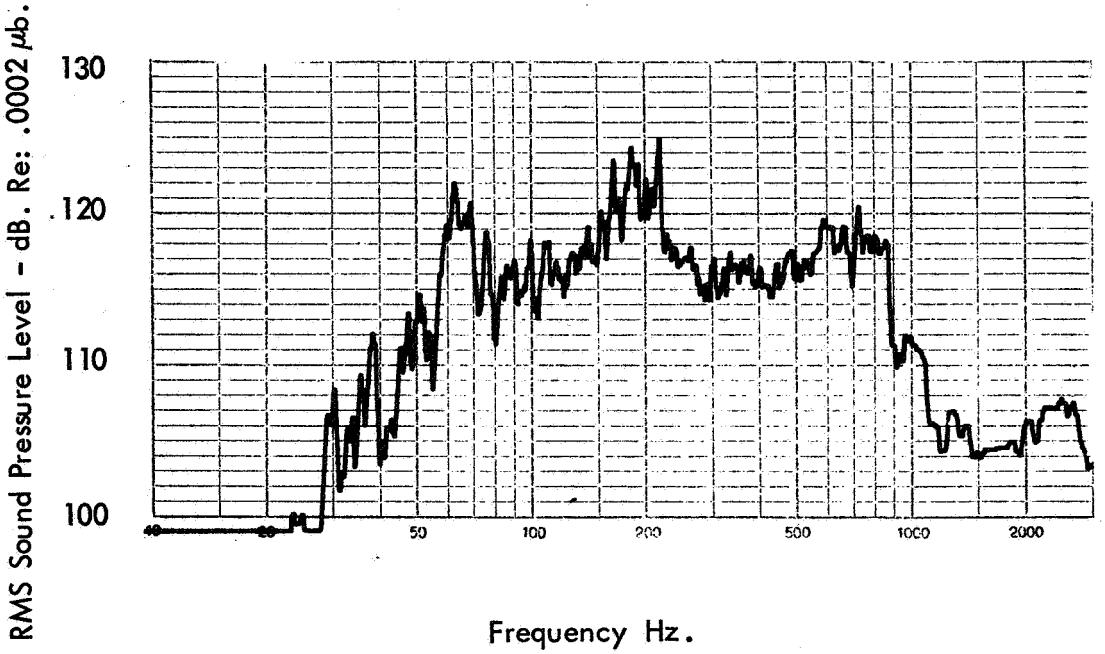

FIGURE 3.17 SOUND PRESSURE LEVEL SPECTRUM OF MICROPHONE M5

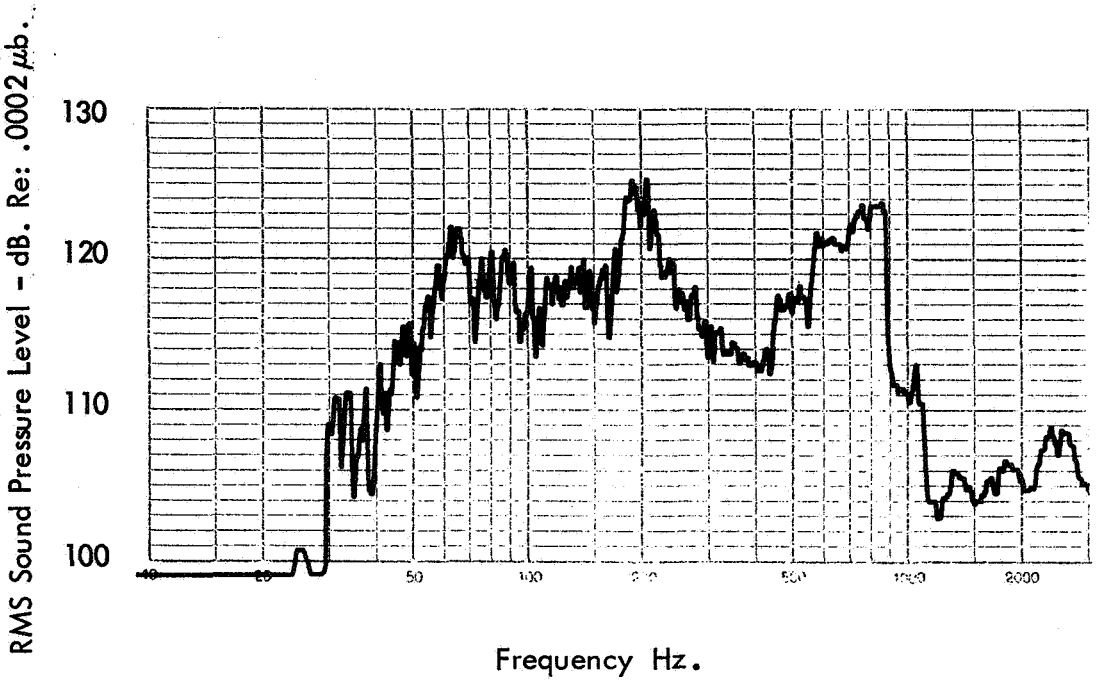

FIGURE 3.18 SOUND PRESSURE LEVEL SPECTRUM OF MICROPHONE M3

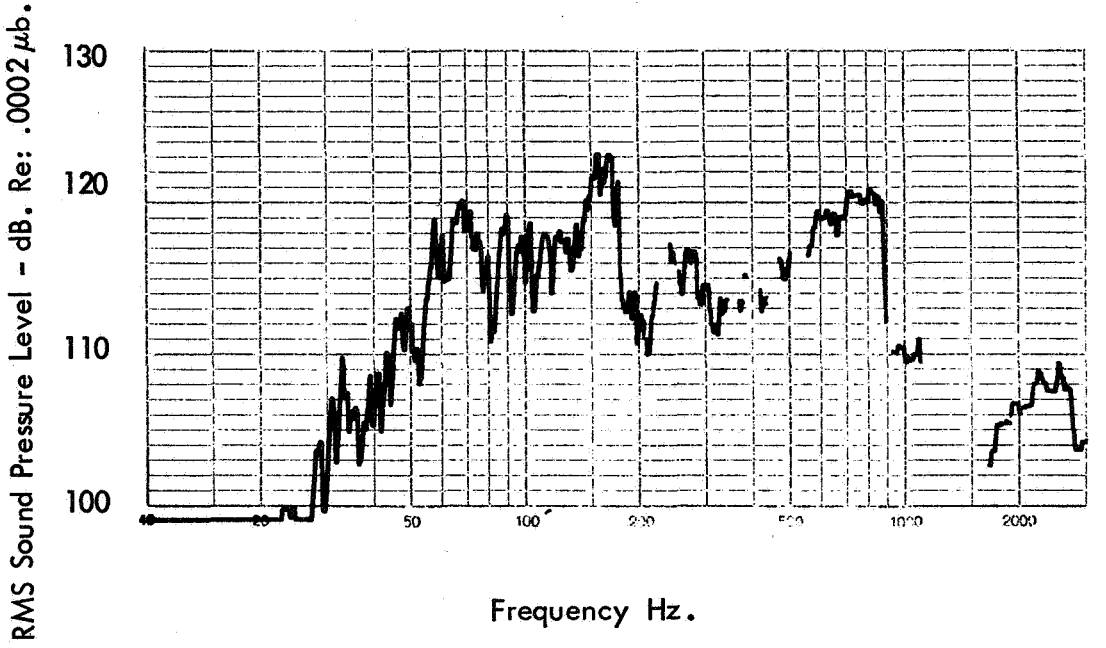

FIGURE 3.19 SOUND PRESSURE LEVEL SPECTRUM OF MICROPHONE M6